NEOPLASIA
www.neoplasia.com

Volume 18 Number 3 March 2016 pp. 185–198 185

Regulation of Glioblastoma Tumor-Propagating Cells by the Integrin Partner Tetraspanin CD151[1,2]

Jessica Tilghman[*,†], Paula Schiapparelli[‡], Bachuchu Lal[*,§], Mingyao Ying[*,§], Alfredo Quinones-Hinojosa[†,‡,¶], Shuli Xia[*,§] and John Laterra[*,†,§,¶]

*Hugo W. Moser Research Institute at Kennedy Krieger, Baltimore, MD, 21205, USA; [†]Department of Neuroscience, Johns Hopkins School of Medicine, Baltimore, MD, 21205, USA; [‡]Department of Neurosurgery, Johns Hopkins School of Medicine, Baltimore, MD, 21205, USA; [§]Department of Neurology, Johns Hopkins School of Medicine, Baltimore, MD, 21205, USA; [¶]Department of Oncology, Johns Hopkins School of Medicine, Baltimore, MD, 21205, USA

Abstract

Glioblastoma (GBM) stem cells (GSCs) represent tumor-propagating cells with stem-like characteristics (stemness) that contribute disproportionately to GBM drug resistance and tumor recurrence. Understanding the mechanisms supporting GSC stemness is important for developing therapeutic strategies for targeting GSC-dependent oncogenic mechanisms. Using GBM-derived neurospheres, we identified the cell surface tetraspanin family member CD151 as a novel regulator of glioma cell stemness, GSC self-renewal capacity, migration, and tumor growth. CD151 was found to be overexpressed in GBM tumors and GBM neurospheres enriched in GSCs. Silencing CD151 inhibited neurosphere forming capacity, neurosphere cell proliferation, and migration and attenuated the expression of markers and transcriptional drivers of the GSC phenotype. Conversely, forced CD151 expression promoted neurosphere self-renewal, cell migration, and expression of stemness-associated transcription factors. CD151 was found to complex with integrins α3, α6, and β1 in neurosphere cells, and blocking CD151 interactions with integrins α3 and α6 inhibited AKT phosphorylation, a downstream effector of integrin signaling, and impaired sphere formation and neurosphere cell migration. Additionally, targeting CD151 *in vivo* inhibited the growth of GBM neurosphere-derived xenografts. These findings identify CD151 and its interactions with integrins α3 and α6 as potential therapeutic targets for inhibiting stemness-driving mechanisms and stem cell populations in GBM.

Neoplasia (2016) 18, 185–198

Introduction

Glioblastoma (GBM) is the most common and aggressive brain malignancy. Despite advances in therapy, improvement in overall survival has been limited. Patients with GBM almost uniformly experience relapse and have a median survival time of only 15 to 20 months despite aggressive treatment with surgery, radiation, and chemotherapy [11,35]. GBM recurrence appears to be disproportionately dependent upon tumor-propagating GBM stem cells (GSCs), which comprise a minority population of highly tumorigenic cells that display stem cell properties (i.e., stemness), including the ability to self-renew as spheres and the capacity to differentiate into multiple neural lineages [15,20,29,33,44,45]. Most importantly, GSCs efficiently propagate tumor xenografts that recapitulate the

Address all correspondence to: John Laterra, MD, PhD, The Kennedy Krieger Institute, 707 N. Broadway, Baltimore, MD 21205.
E-mail: laterra@kennedykrieger.org

[1] Disclosure of potential conflicts of interest: The authors indicate no potential conflicts of interest.

[2] Grant support: This work was partially funded by National Institutes of Health RO1NS076759 (J. L.) and RO1NS070024 (A. Q. H.), the National Science Foundation Graduate Research Fellowship Program (J. T.), and the Ford Foundation Predoctoral Fellowship Program (J. T.).
Received 3 November 2015; Revised 29 January 2016; Accepted 9 February 2016

1476-5586
http://dx.doi.org/10.1016/j.neo.2016.02.003

biological and histopathological characteristics of their original tumor when implanted orthotopically [29,51]. These cells use microenvironment-dependent and -independent mechanisms to promote tumor angiogenesis, recurrence, and resistance to cytotoxic therapies [2,48,50,51]. Understanding the mechanisms supporting GSCs and their tumor-propagating behaviors is important for developing novel and more effective therapies.

CD151 is a member of the integral membrane protein superfamily tetraspanins. CD151 interacts with multiple proteins at the cell surface, particularly the laminin-binding integrins α3, α6, β1, and β4, to modulate their intracellular signaling and contribute to the regulation of cell adhesion and migration [47,53,63]. The tetraspanins are also involved in cell proliferation and tissue vascularization [37,38,60,61]. CD151 is highly expressed in several cancers, including gastric, endometrial, liver, breast, prostate, and glioma [9,10,52,55,56]. Its aberrant expression is associated with multiple oncogenic activities such as metastasis and angiogenesis [8,10].

CD151 has been associated with glioma malignancy, but its mechanisms of action remain poorly defined. A retrospective single-institution study of Asian patients with newly diagnosed GBM found that tumors expressing high levels of CD151 were associated with shorter progression-free and overall survival [28]. CD151 expression has been associated with a network of oncogenic myc-interacting genes in glial malignancies [5]. Rao Malla et al. [40] have implicated CD151 in the mechanism by which urokinase-type plasminogen activator receptor and cathepsin regulate cell adhesion and invasion.

A role for CD151 in regulating cell stemness and cancer stem cells remains undefined. Yin et al. [58] found that CD151 knockout increased the differentiation potential of mammary luminal stem and progenitor cell subtypes, suggesting a role in modulating mammary cell multipotency and differentiation signals. We recently reported a potentially related finding that *CD151* is among a network of genes that are repressed by KLF9, a transcription factor that drives GSC differentiation [27,59]. High CD151 expression has been found to mark tumor-propagating prostate cells and CD133+ tumorigenic colon cancer cell lines [18,39]. Furthermore, integrin α6, which marks and regulates GBM stem cells, is known to associate with cell surface CD151 [27,59]. There are currently no reports directly linking CD151 expression and/or function to tumor-propagating GSCs.

It is within this context that we investigated the expression and function of CD151 in tumor-propagating GSCs. CD151 was found to be highly expressed in glial tumors and GBM neurosphere isolates. Silencing endogenous CD151 inhibited glioma cell stemness and GSC self-renewal, migration, and xenograft growth. Transgenic CD151 expression enhanced these phenotypic properties. CD151 was found to associate with integrins α3, α6, and β1 in GSCs, and blocking CD151 integrin interactions inhibited sphere formation, migration, and activation of downstream integrin signaling. Together, these results identify CD151 and direct interactions between CD151 and integrins as potential therapeutic targets in GSCs.

Materials and Methods

Reagents

All reagents were purchased from Sigma-Aldrich unless otherwise stated. Doxycycline (Dox) was diluted to a concentration of 1 μg/ml in cell culture medium as a working concentration. In all experiments, the final DMSO concentration was <0.1%, which had no demonstrable effect on neurosphere cultures. Laminin was diluted to 10 μg/ml as a working concentration unless otherwise indicated.

Cell Culture

Human GBM neurosphere lines 0913 (GBM1A) and 0627 (GBM1B) were originally established by Vescovi and colleagues [15] and further characterized by us [31,49,59]. The 1123 (M1123) and 146 (P146) neurosphere lines were derived from high-grade glioma patients and kindly provided by Dr. Nakano (Ohio State University). Primary GBM neurospheres JHH612 (612) were derived from a clinical GBM specimen at Johns Hopkins University using the methods and culture conditions described by Galli et al. [15]. Neurospheres were cultured in serum-free medium supplemented with epidermal growth factor and fibroblast growth factor and incubated in 5% CO_2/95% air condition at 37°C. Primary neurospheres were used at less than 10 passages. All human materials were obtained and used in compliance with The Johns Hopkins Institutional Review Board.

Lentiviral Transduction

The sequences for CD151 shRNA lentiviral vectors (TRCN0000300360, TRCN0000300331; Sigma-Aldrich; V3THS_308057; Thermo Scientific, Hudson, NH, www.thermoscientific.com) are listed in Supplementary Table S1. N-terminal 3xFLAG-tagged CD151 (3F-CD151) was constructed by high-fidelity polymerase chain reaction (PCR; Roche, Basel, Switzerland, www.roche-applied-science.com) and cloned into the pTRIPZ vector (Thermo Scientific) using *Age*I and *Mlu*I restriction sites. The Trans-Lentiviral Packaging System (Thermo Scientific) was used for lentivirus production. Cells were transfected with lentivirus at a multiplicity of infection of 5 for 24 hours with TransDux Virus Infection solution (System Biosciences, Mountain View, CA, www.systembio.com). Stable GBM neurosphere lines were established by puromycin selection (1 μg/ml).

Neurosphere Formation Assays

Viable cells (2×10^3/well or 2×10^4/well) were cultured in 48-well or 6-well plates, respectively. After 7 to 14 days, neurospheres were fixed in medium with 1% agarose, stained with 1% Wright stain solution, and counted by computer-assisted morphometry (MCID software, Cambridge, UK, www.mcid.co.uk) by measuring the number of neurospheres (>50 μm or >100 μm in diameter, as indicated) in three random fields per well.

Flow Cytometric Assay

Flow cytometric analysis was performed on unfixed cells stained with anti-CD133/2(AC133)-phycoerythrin (PE) (Miltenyi Biotec, Auburn, CA, www.miltenyibiotec.com) or PE-CD151 (BD Biosciences, San Jose, CA, www.bdbiosciences.com) antibody following the manufacturer's protocol using a FACSCalibur (BD Biosciences). Mouse IgG labeled with PE or FITC was used as a control.

Western Blot Analysis

Total cellular protein was extracted with radioimmunoprecipitation assay buffer (Sigma-Aldrich) containing protease and phosphatase inhibitors (Calbiochem, Billerica, MA, www.calbiochem.com). The Subcellular Protein Fractionation Kit was used for membrane protein extraction (Thermo Scientific). SDS-PAGE was performed with 50 μg of

total proteins using 4% to 12% gradient Tris-glycine gels (LI-COR Biosciences, Lincoln, NE, www.licor.com). Western blot analysis was performed using the Quantitative Western Blot System, with secondary antibodies labeled by IRDye infrared dyes (LI-COR Biosciences). The primary antibodies were anti-CD151, anti-Olig2, anti-FLAG (Santa Cruz), anti-Sox2, anti-S^{473}-pAkt, anti-total-Akt, anti-integrin α3, anti-integrin α6, anti-integrin β1 (Cell Signaling), anti-pan Cadherin (Abcam, Cambridge, MA, www.abcam.com), and anti-β-actin (Sigma-Aldrich).

Immunoprecipitation

A total of 1×10^7 GBM1A 3F-CD151 cells were treated ± Dox for 48 hours. Cells were lysed in the immunoprecipitation buffer containing 1% Brij-O1, 20 mM Tris HCl pH 8, 137 mM NaCl, 2 mM EDTA, and protease and phosphatase inhibitors (Calbiochem) for 1 hour at 4°C on a rotating shaker. Anti-FLAG M2 magnetic beads (Sigma-Aldrich) or protein A/G magnetic beads as control were added to the above cell lysate and incubated overnight at 4°C on a rotating shaker. Beads were collected, and 3F-CD151 bound complexes were eluted using 3× FLAG peptide (Sigma-Aldrich). Immunoprecipitates were immunoblotted with primary antibodies.

Immunofluorescence

Neurosphere cells were collected by cytospin onto glass slides and fixed with 4% paraformaldehyde. Cells were permeabilized by Triton X-100 and immunostained with anti-CD151 (1:50; Santa Cruz Biotechnology, Dallas, TX, www.scbt.com), anti-integrin α3 (1:50), anti-integrin α6 (1:50), and anti-integrin β1 (1:100; Cell Signaling) antibodies following the protocol from Cell Signaling. Secondary antibodies were conjugated with Alexa488 or Cy3 (1:250). Immunofluorescent images were taken and analyzed using the ZEISS AxioImager M2 Imaging System with Axiovision software (Zeiss, Thornwood, NY, www.zeiss.com).

Cell Adhesion Assays

Neurosphere cells were dissociated and plated on laminin-coated wells for 2 and 6 hours. Adherent cells were fixed with 4% paraformaldehyde and washed with 0.1% BSA/phosphate-buffered saline. The fixed cells were stained with crystal violet, dissolved with 2% SDS, and quantified spectrophotometrically at 550 nm using a SpectraMAX 340pc (Molecular Devices, Sunnyvale, CA, www.moleculardevices.com) plate reader. Results show relative adhesion measured after subtracting the background absorbance from all values.

Cell Migration Assays

Cell migration assays were performed using laminin-coated Transwell chambers. The upper chamber medium consisted of neurosphere culture medium without epidermal growth factor/fibroblast growth factor, and the lower chamber medium consisted of Dulbecco's modified Eagle's medium (DMEM) with 10% FBS. After 8 hours, cells that had migrated through the filter were fixed and stained with Hoechst 33342 (Life Technologies). Migration was quantified by counting cells from eight random fields. Migration of glioma cells was also quantified using a directional migration assay using a multiwell nanopatterned device, consisting of parallel nanoridges/grooves of 400 nm in groove width, 400 nm in ridge width, and 500 nm in depth, constructed of transparent poly(urethane acrylate) and fabricated using UV-assisted capillary lithography as previously described [22,23]. Before plating cells, nanogrooved substrata were coated with poly-D-ornithine (10-μg/ml concentration) for 15 minutes and laminin (3 $\mu g/cm^2$) overnight. These topographically patterned cell substrata cause cells to align with and move along the direction of the nanogrooves. Cell migration was quantified using time-lapse microscopy and a motorized inverted microscope (Olympus IX81) equipped with a Cascade 512B II CCD camera and temperature- and gas-controlling environmental chamber. Phase-contrast cell images were automatically recorded under 4*1.6× objective using the Slidebook 4.1 (Intelligent Imaging Innovations, Denver, CO) for 10 hours at 10-minute intervals as previously published by us [13,14,17,25,30,46,62]. A custom-made MATLAB script was used to calculate cell speed using time-lapse microscopy data as described previously [1,17,25,30]. The average speeds of individual cells were calculated from the total distance moved throughout the entire cell trajectory and total recording time.

Tumor Implantation and Animal Treatments

All animal protocols were approved by the Johns Hopkins School of Medicine Animal Care and Use Committee. For subcutaneous (s.c.) xenografts, female athymic nude mice were injected s.c. in the flank with 5×10^6 viable neurosphere cells (determined by Trypan blue exclusion) in 0.1 ml of DMEM. When tumors reached about 50 mm^3, mice were randomly divided into groups for treatment. Dox was administered in animal feed. Tumor sizes were determined daily by measuring two dimensions (length [*a*] and width [*b*]), and volumes (*V*) were calculated using the formula $V = ab^2/2$ [26].

For intracranial (i.c.) xenografts, severe combined immunodeficiency (SCID) mice received 5000 viable neurosphere cells in 2 μl of DMEM by stereotactic injection to the right caudate/putamen (anterior-posterior = 0 mm, mesial-lateral = −2.5 mm, dorsal-ventral = −3.0 mm). Mice were perfused with 4% paraformaldehyde at the indicated times, and the brains were removed for histological analysis. Tumor sizes were quantified by measuring maximum tumor volume on hematoxylin and eosin–stained brain coronal sections using computer-assisted morphometry (MCID software).

Quantitative Real-Time PCR (qRT-PCR)

Total RNA was extracted using Rneasy Mini Kit (Qiagen, Venlo, Limburg, www.qiagen.com). After reverse transcription using MuLV reverse transcriptase (Applied Biosystems, Calsbad, CA, www.appliedbiosystems.com) and Oligo(dT) primer, qRT-PCR was performed using SYBR Green PCR Mix (Applied Biosystems) and IQ5 detection system (Bio-Rad, Hercules, CA, www.bio-rad.com). Primer sequences are listed in Supplementary Table S1. Relative gene was normalized to 18S rRNA.

Statistical Analysis

Statistical analysis was performed using Prizm software (GraphPad, La Jolla, CA, www.graphpad.com). *Post hoc* tests included the Student's *t* test and Tukey multiple comparison tests as appropriate. All data are represented as mean value ± SEM unless otherwise indicated.

Results

High Expression of CD151 in Aggressive Glioma Subtypes and GSCs

The Repository for Molecular Brain Neoplasia Data (REMBRANDT) database (National Cancer Institute, https://cairegrator.nci.nih.gov/rembrandt/), representing 28 nonneoplastic brain and 443 glioma tissue samples, was used to compare the expression profile of CD151 in normal brain and glioma tissues. CD151 expression was found to be 4.9-, 2.1-,

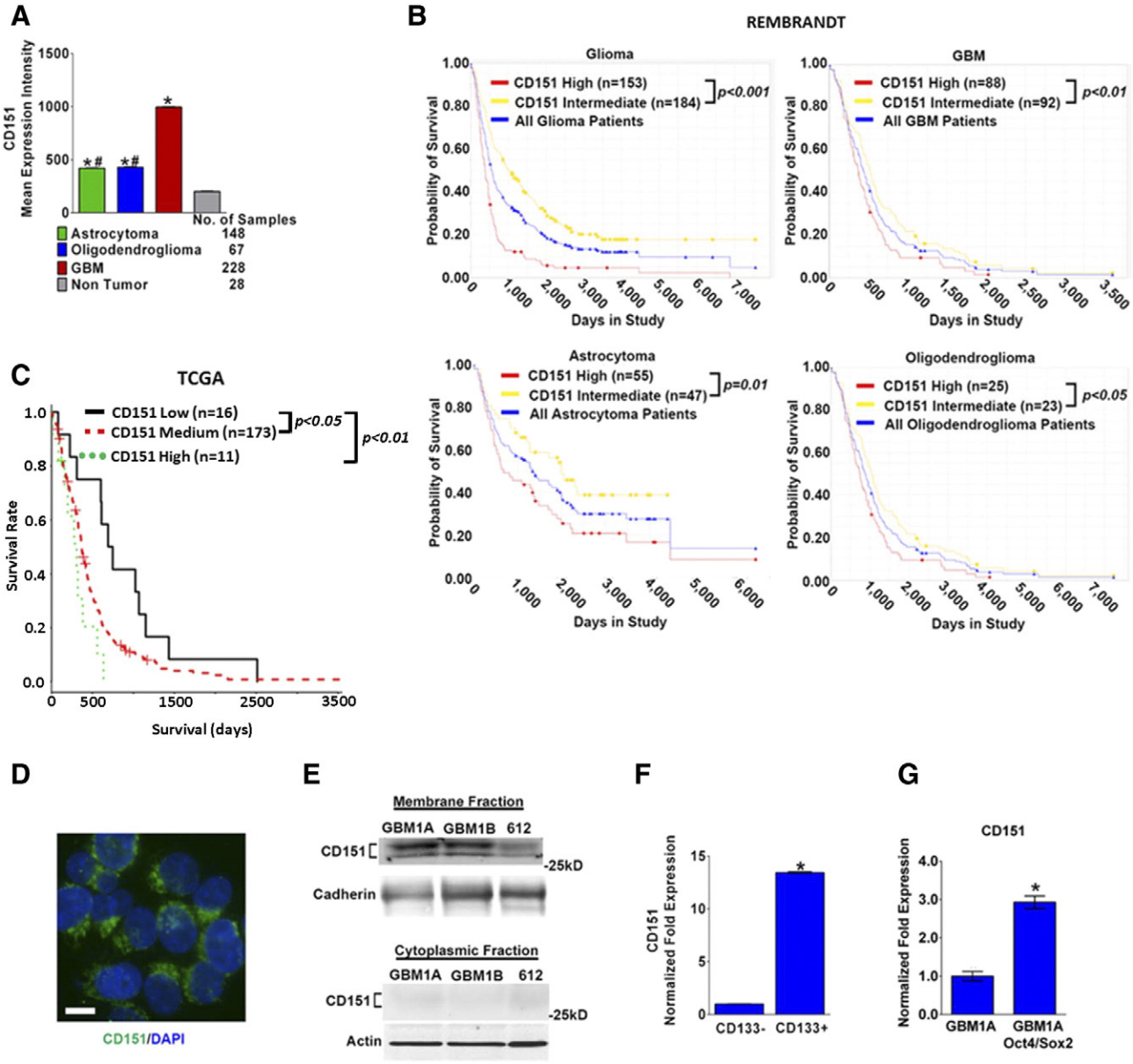

Figure 1. CD151 is highly expressed in glioma and GSCs.(A) CD151 mean gene expression intensity from REMBRANDT database (*,#$P <$ .0001 compared with nonneoplastic brain or GBM, respectively). CD151 expression is significantly upregulated in glioblastoma multiforme (GBM) samples when compared with nonneoplastic brain, oligodendroglioma, or astrocytoma samples. (B and C) Kaplan-Meier survival plots for glioma patients based on differential gene expression of CD151 from REMBRANT (B) and TCGA (C) databases. The probability of survival is significantly lower in samples with high CD151 gene expression compared with samples with intermediate expression in all glioma, GBM, astrocytoma, and oligodendroglioma samples. For REMBRANDT comparisons, high CD151 gene expression samples were up at least two-fold in all glioma, astrocytoma, and oligodendroglioma samples and at least six-fold in GBM compared with intermediate samples. Inclusion of patients with low CD151 expression was not possible because of insufficient sample size. For TCGA comparisons, high CD151 expression samples were at least three-fold higher and low samples not more than three-fold lower than intermediate samples. (D) Fluorescent photomicrography of GBM1B neurospheres permeabilized with Triton X-100 and immunostained using anti-CD151 antibody (green fluorescence). Blue fluorescence indicates 4',6-diamidino-2-phenylindole) (4',6-diamidino-2-phenylindole (DAPI) nuclear stain (bar = 10 μm). (E) Membrane and cytoplasmic protein fractions isolated from GBM neurosphere lines (GBM1A, GBM1B) and primary GBM neurosphere (612) were subjected to immunoblot analysis with anti-CD151 antibody. CD151 localizes to membrane but not the cytoplasm of glioma stem cells. (F) GBM1A neurosphere cells expressing undetectable and high levels of CD133 (CD133 − and CD133 +, respectively) were separated by flow cytometry. qRT-PCR analysis shows that CD151 mRNA expression is significantly higher in CD133 + cells (*$P <$ .01). (G) CD151 expression was analyzed by qRT-PCR in GBM1A and GBM1A cells overexpressing stemness-driving transcription factors Oct4 and Sox2 (GBM1A Oct4/Sox2). CD151 mRNA expression is higher in GBM1A Oct4/Sox2 cells compared with GBM1A cells. *$P <$ .05.

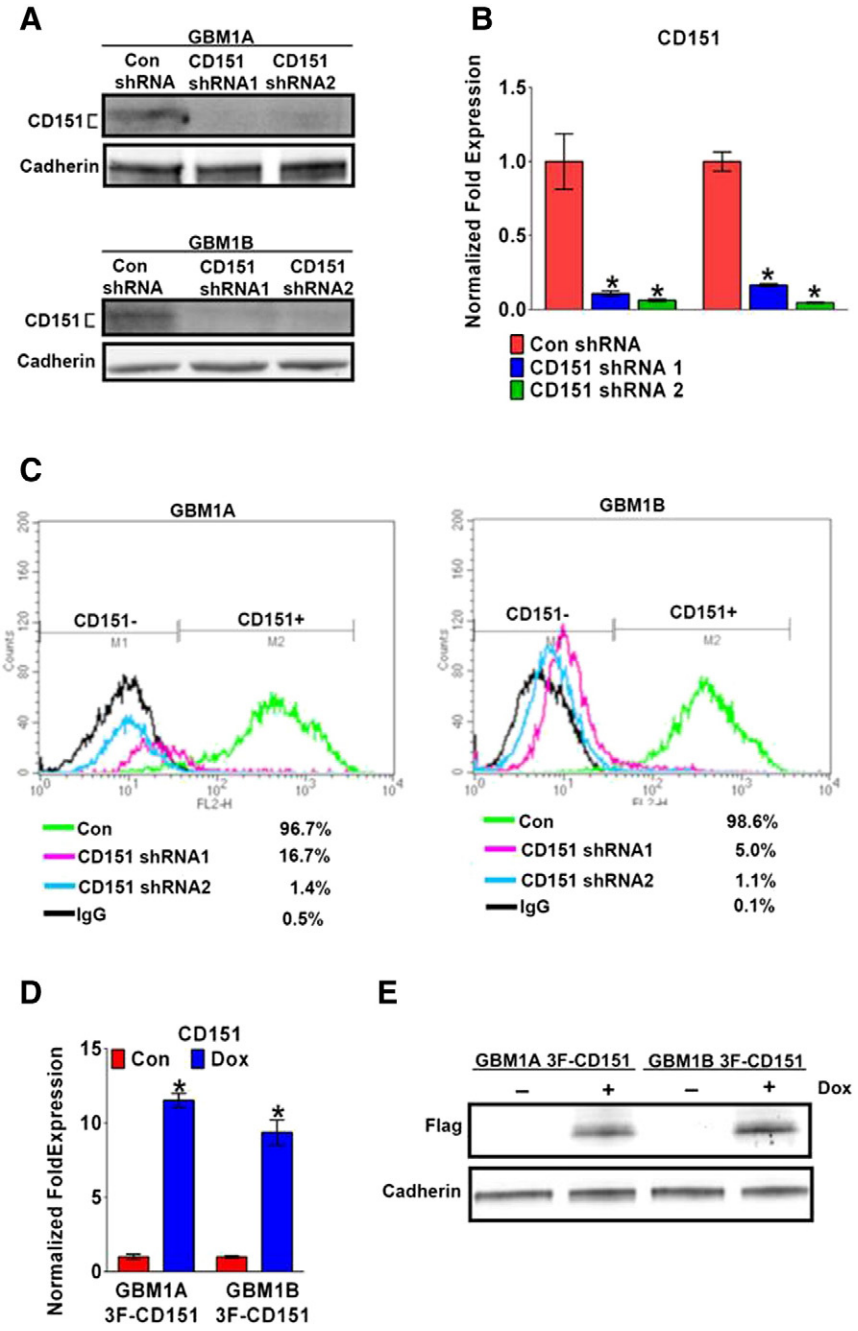

Figure 2. CD151 knockdown and transgenic CD151 expression in glioma neurospheres.(A–C) GBM neurospheres (GBM1A and GBM1B) were infected with lentivirus coding for control shRNA, CD151 shRNA 1, or CD151 shRNA 2 (sequences provided in Supplemental Table 1). CD151 expression was quantified by (A) immunoblot analysis of membrane protein collected 72 hours later using anti-CD151 antibody and (B) qRT-PCR analysis of whole cell mRNA. (C) Neurosphere cells were analyzed by flow cytometry 6 days after transduction with lenti-CD151 shRNA using CD151 antibodies and isotype IgG control. CD151 knockdown significantly reduced the number of CD151 + cells. Representative histograms and the percentages of CD151 + cells are shown. (D and E) GBM-derived neurosphere cells expressing a Dox-inducible 3FLAG-tagged CD151 (GBM1A 3F-CD151 and GBM1B 3F-CD151) were treated ± Dox for 48 hours. 3Flag-CD151 expression was analyzed by qRT-PCR using *CD151*-specific primers (D) and immunoblot of cell membrane fractions using anti-Flag (E). *$P < .001$.

and 2.1- fold higher in GBM, oligodendroglioma, and astrocytoma compared with nonneoplastic brain samples, and 2.3- and 2.4-fold higher in GBM samples compared with oligodendroglioma and astrocytoma samples, respectively (Figure 1*A*).

To investigate potential correlations between CD151 expression and clinical outcome, we analyzed the prognostic significance of CD151 in the REMBRANDT samples using Kaplan-Meir survival curve analysis with log-rank comparisons. Survival for patients expressing upregulated CD151 was significantly shorter compared with that in those with intermediate expression in all glioma and specific glioma subtypes ($P < .001$, $P = .008$, $P = .027$, and $P = .012$ in all glioma, GBM, oligodendroglioma, and astrocytoma samples,

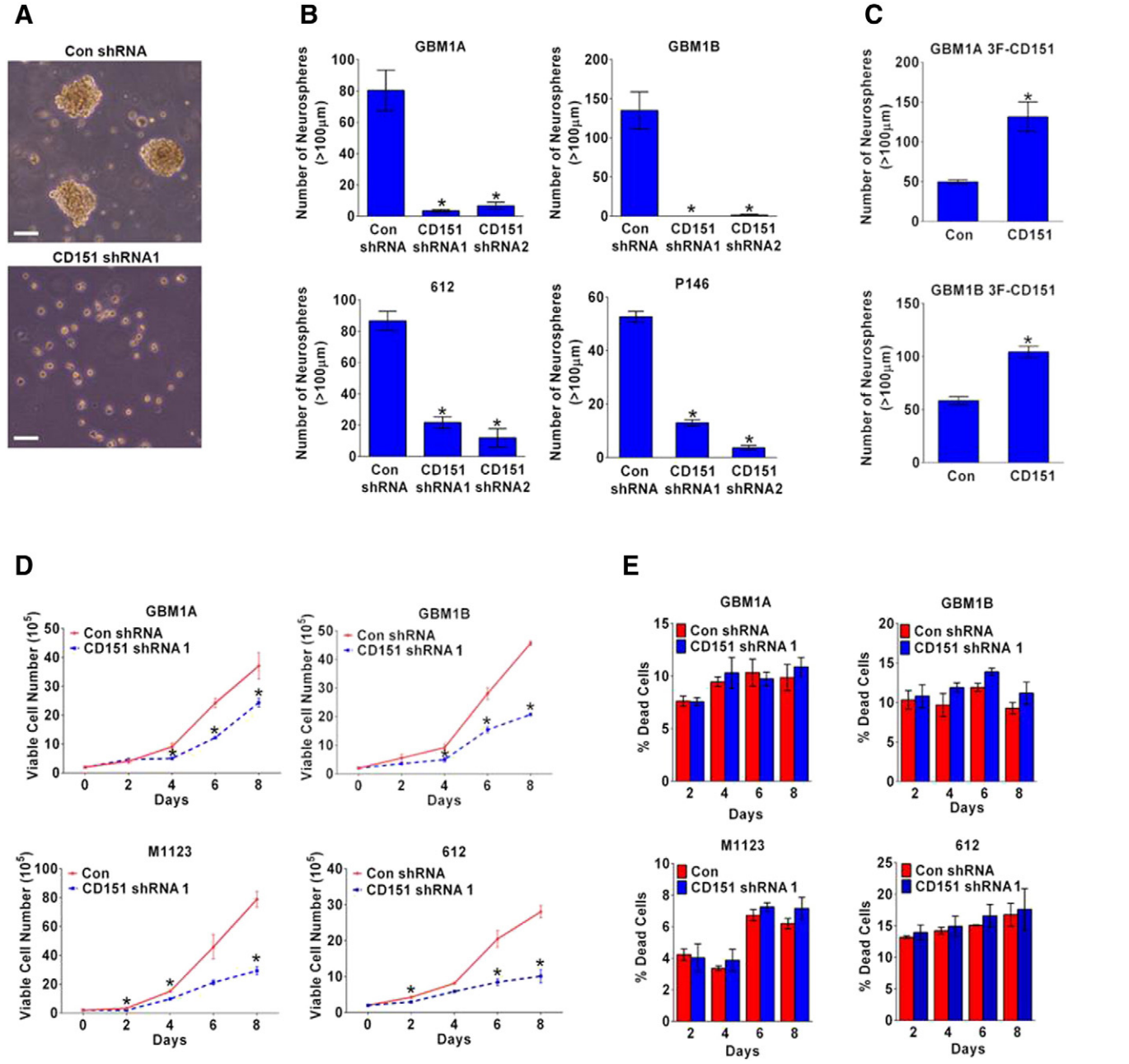

Figure 3. CD151 regulates GSC self-renewal,(A and B) GBM neurosphere lines (GBM1A, GBM1B, P146) and primary GBM neurospheres (612) were infected with lentivirus coding for control shRNA, CD151 shRNA 1, or CD151 shRNA 2. Equal numbers of viable cells were plated and cultured for 14 days posttransduction to allow neurosphere formation. (A; bar = 100 μm) Representative microscopic images of GBM1B neurospheres with control or CD151 shRNA are shown. (B) Neurospheres (>100 μm diameter) were counted. CD151 silencing inhibited neurosphere formation in all neurosphere isolates examined. (C) Equal numbers of GBM1A 3F-CD151 and GBM1B 3F-CD151 neurosphere cells were plated and cultured for 7 days ± Dox under neurosphere growth conditions. Neurospheres (>100 μm diameter) were quantified. CD151 overexpression increased neurosphere formation. (D and E) GBM1A, GBM1B, M1123, and 612 neurosphere cells infected with lentivirus coding for control shRNA, CD151 shRNA 1, or CD151 shRNA 2 and cultured under neurosphere growth conditions. Dissociated cells were stained with Trypan blue, and both viable (unlabeled) and nonviable (labeled) cells were counted on the days indicated posttransduction. CD151 knockdown inhibited cell growth (D) but did not alter cell viability (E). *$P < .05$ compared with controls.

respectively, log-rank test) (Figure 1*B*). The numbers of "low" CD151-expressing tumors were insufficient to compare with other groups. A similar statistically significant correlation between high CD151 expression and poor survival was identified using The Cancer Genome Atlas (TCGA) glioblastoma dataset (National Cancer Institute, https://tcga-data.nci.nih.gov/tcga) (Figure 1*C*).

We examined CD151 expression in GBM-derived neurosphere lines (GBM1A and GBM1B) and low passage GBM-derived primary neurospheres (612) enriched in GSCs. Immunostaining readily detected CD151 expression (Figure 1*D*) that was found by immunoblot to localize to membrane but not cytoplasmic fractions in multiple GSC lines (Figure 1*E*). CD151 expression was further examined by qRT-PCR analysis of

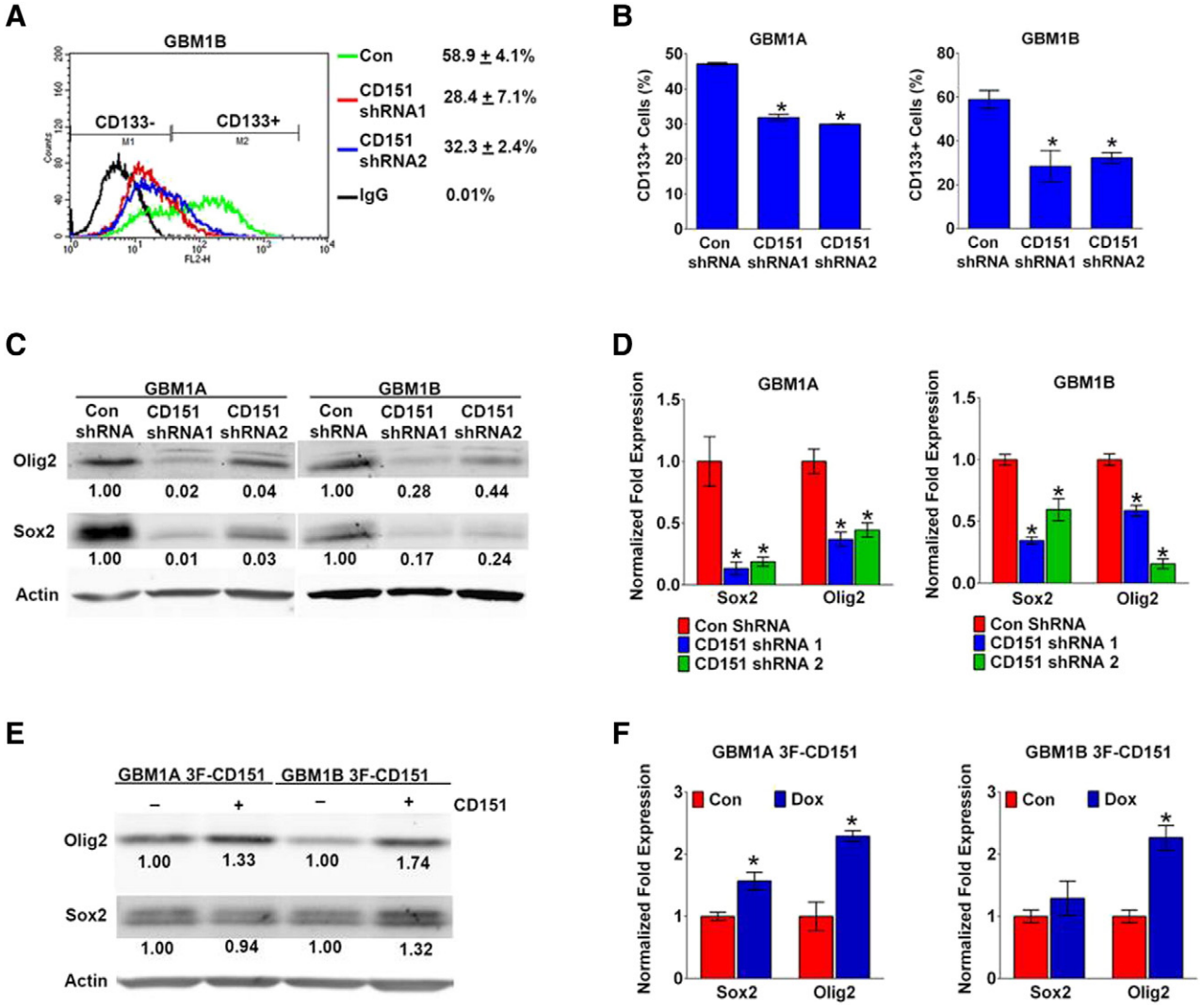

Figure 4. CD151 expression regulates expression of GSC markers and transcription factors.(A–D) GBM1A and GBM1B neurospheres were infected with lentivirus coding for control shRNA, CD151 shRNA 1, or CD151 shRNA 2. (A and B) GBM1A and GBM1B cells were analyzed by flow cytometry 6 days posttransduction using anti-CD133 and isotope IgG control. A representative histogram and the percentages of CD133+ cells are shown. CD151 silencing decreased the number of CD133+ cells. Total cell lysates were analyzed by immunoblot (C) and by qRT-PCR (D) for Sox2 and Olig2 expression. CD151 inhibition decreased expression of Sox2 and Olig2. (E and F) GBM1A 3F-CD151 and GBM1B 3F-CD151 neurospheres expressing Dox-inducible 3Flag-CD151 were treated ± Dox. Whole cell extracts were analyzed by immunoblot for Olig2 and Sox2 (E). Transgenic CD151 expression promoted Olig2 expression in both cells and Sox2 expression in GBM1B 3F-CD151 GSCs. Analysis of Sox2, and Olig2 expression by qRT-PCR shows that CD151 promoted mRNA expression of the stemness-driving transcription factors (F).

CD133+ neurosphere cell subpopulations, which are widely considered to represent GBM-propagating stem cells [45]. CD151 expression was elevated in CD133+ cells relative to CD133− cells (Figure 1*F*).

To further study the association of CD151 with cell stemness and stemness-driving transcription factors, CD151 expression was analyzed using qRT-PCR in GBM-derived neurospheres engineered to overexpress Oct4 and Sox2 (GBM1A Oct4/Sox2). Co-expressing transgenic Oct4 and Sox2, previously shown by us to induce tumor-propagating GSCs [34], increased CD151 expression three-fold (Figure 1*F*). These results show that CD151 is upregulated in the most aggressive gliomas and that CD151 upregulation is associated with poor prognosis independent of glioma grade. CD151 expression is also highly upregulated in glioma-propagating stem cells.

Regulation of GSC Self-Renewal by CD151

Gain- and loss-of-function approaches were used to evaluate the effects of CD151 expression in GSCs. Transduction of GBM-derived neurospheres with lentivirus coding for CD151 shRNAs (CD151 shRNA 1 and CD151 shRNA 2) significantly inhibited CD151 protein and mRNA expression (Figure 2, *A* and *B*) and decreased the number of CD151+ cells by up to 99% (Figure 2*C*). We also engineered three independent neurosphere lines to express a Dox-inducible N-terminal 3xFLAG-tagged CD151 transgene (3F-CD151; designated as GBM1A 3F-CD151, GBM1B 3F-CD151, and 612 3F-CD151). Dox treatment for 48 hours induced expression of CD151 mRNA and membrane-associated CD151 protein (Figure 2, *D* and *E*).

The effects of CD151 silencing on GSC self-renewal and cell proliferation were examined. Self-renewal as measured by neurosphere formation was markedly inhibited by CD151 expression knockdown (61% to 96% inhibition) in multiple lines and primary isolates, including neurospheres derived from mesenchymal (M1123) and proneural (P146) glioblastoma subtypes (Figure 3, *A* and *B*; Fig. S1). Conversely, forced CD151 expression significantly increased neurosphere formation (Figure 3*C*). Silencing CD151 expression impaired neurosphere cell proliferation from 34% to 63% (Figure 3*D*). CD151 knockdown did not induce detectable cell death (Figure 3*E*).

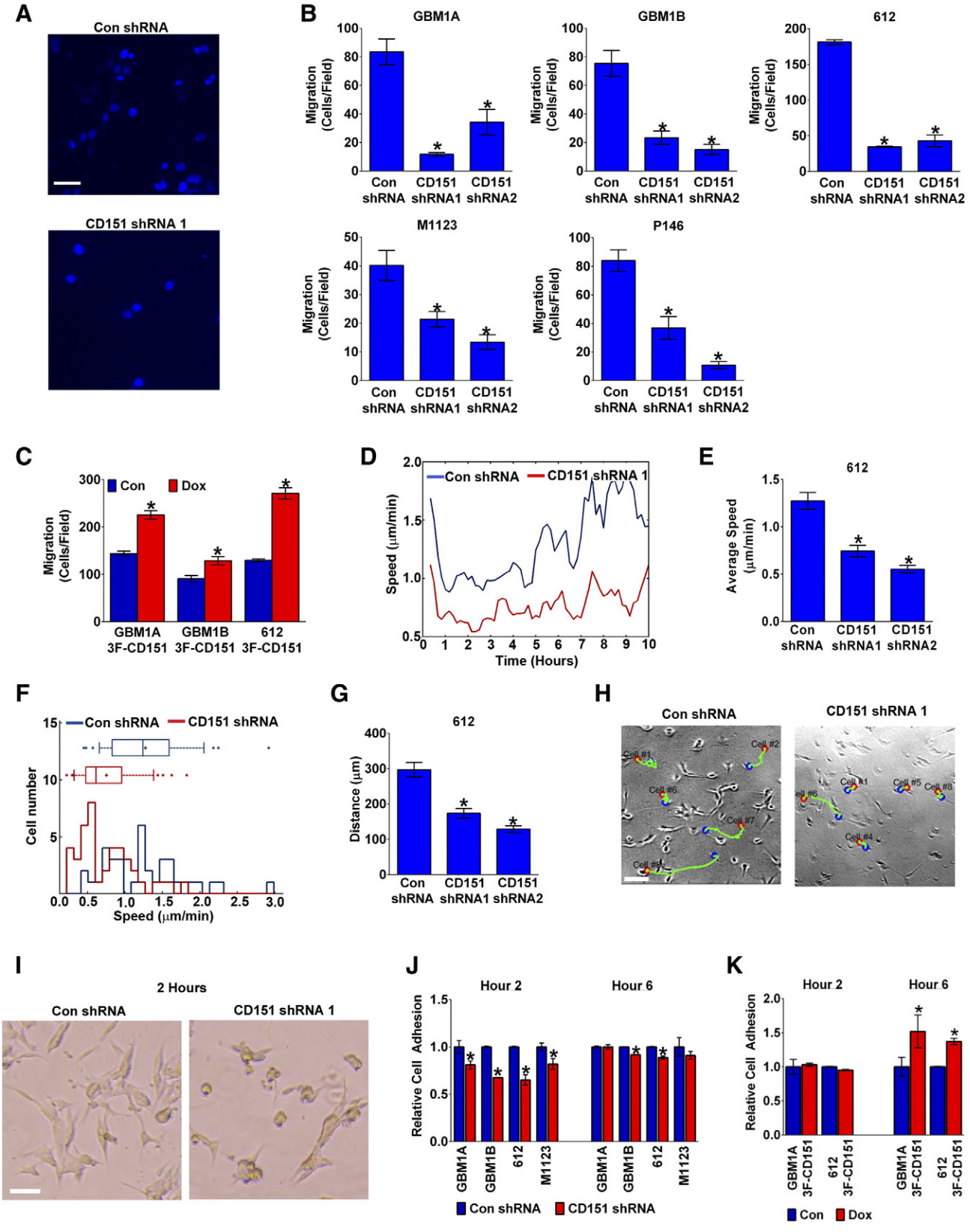

Regulation of Markers and Modulators of Glioma Stemness by CD151

We investigated the effect of CD151 silencing on the expression of markers and regulators of GBM cell stemness. CD151 knockdown in neurospheres reduced the number of CD133+ cells by 32% to 52% (Figure 4, *A* and *B*). GSCs are regulated by stemness-associated transcription factors, including Olig2 and Sox2 [16,31,34]. CD151 silencing decreased Sox2 and Olig2 expression as evidenced by reductions in both cellular RNA and protein (Figure 4, *C* and *D*). Conversely, there was a variable but strong trend of increased Olig2 and Sox2 expression in response to forced CD151 expression (Figure 4, *E* and *F*).

Inhibition of GBM Neurosphere Cell Adhesion and Migration by CD151 Targeting

GBM-derived neurosphere cells transduced with control lentivirus or with lentiviral vectors engineered to express either CD151 shRNA were seeded on laminin-coated Transwell membranes to evaluate migration capacity. CD151 silencing reduced migration by 47% to 87% (Figure 5, *A* and *B*). Conversely, forced CD151 expression enhanced cell migration on laminin-coated Transwells by 42% to 109% (Figure 5*C*).

The glioma microenvironment constitutes a physically and chemically diverse terrain that influences cell migration. Specifically, glioma cells preferentially migrate along structured pathways such as myelinated neuronal tracts and blood vessels [4]. To further study the effect of CD151 on architecturally directed GSC migration, neurosphere cells transfected with control or CD151 shRNA lentivirus were seeded on a laminin-coated substrate consisting of linear nanoscale grooves. Migration along the nanoscale grooves enables a more precise assessment of migration parameters such as cell speed and distance traveled over several hours. CD151 silencing significantly reduced average cell migration speed by 41% to 57% (Figure 5, *D* and *E*; Video S1). In addition, control shRNA transfected cells showed a higher percentage of cells migrating at maximum speeds than CD151 shRNA transfected cells (Figure 5*F*). CD151 knockdown also reduced the average distance migrated over 10 hours (Figure 5, *G* and *H*).

Cell adhesion events impact cell migration capacity. To determine if CD151 modulates neurosphere cell adhesion, GBM-derived neurosphere cells transduced with control lentivirus or lentivirus coding for CD151 shRNA were seeded on a laminin-coated substrata. CD151 silencing delayed the rate of cell adhesion and spreading (Figure 5, *I* and *J*). Forced CD151 expression had no effect on cell adhesion when evaluated 2 hours after seeding on a laminin-coated surface but significantly increased adhesion after 6 hours (Figure 5*K*). Collectively, the data indicate that CD151 regulates neurosphere cell adhesive and migratory interactions with laminin-containing matrices.

Regulation of GBM Neurospheres by CD151-Integrin Interactions

CD151 complexes with laminin-binding integrins and influences integrin-driven biological processes in several cell types [47,53]. Integrins are also highly expressed in stem cells, including GSCs, and thought to contribute to stemness by modulating interactions with micoenvironmental niches [6,27]. Immunofluorescent staining showed that CD151 colocalizes with integrins α3, α6, and β1 in the plasma membrane of GBM neurosphere cells (Figure 6*A*). To further investigate CD151's association with integrins, GBM1A 3F-CD151 neurosphere cells were treated ± Dox for 48 hours to induce CD151 expression. CD151 immunoprecipitation using anti-FLAG co-precipitated integrins α3, α6, and β1 (Figure 6*B*). Neither forced expression of CD151 nor knockdown of endogenous CD151 altered levels of membrane-associated cell surface integrins α6 and β1 (Figs. S2 and 3).

We investigated the effect of CD151 expression on activation of integrin signaling in GBM neurosphere cells. CD151 knockdown reduced serine^{473} Akt phosphorylation, a downstream effector of integrin signaling that promotes various biological processes including survival and cell motility [7], whereas forced CD151 expression enhanced Akt phosphorylation (Figure 6, *C* and *D*).

The anti-CD151 antibody TS151r, previously shown to specifically block interactions between CD151 and integrins α3 and α6 [21,41,47,57], was used to determine if CD151-integrin interactions modulate GSC behavior. Incubating cells with TS151r mimicked CD151 expression knockdown by multiple criteria. TS151r inhibited self-renewal as spheres by 77% to 95% (Figure 6*E*), reduced cell migration on laminin by 70% to 75% (Figure 6*F*), and inhibited Akt phosphorylation (Figure 6*G*). We examined the effect of the Akt inhibitor MK-2206 on the stimulation of GSC migration by CD151 to further examine the role of Akt activation as a downstream effector of CD151-mediated cell responses. MK-2206 was found to reverse GSC migration induction by Dox-inducible CD151 (Figure 6*H*). Taken together, the results strongly support a mechanism by which CD151-laminin interactions support GSC self-renewal and migration by altering integrin function and downstream Akt signaling.

Figure 5. CD151 regulates GBM neurosphere cell adhesion and migration.(A–C) GBM neurospheres (GBM1A, GBM1B, P146, M1123, 612) transduced with lentivirus coding either for control shRNA, CD151 shRNA 1, or CD151 shRNA 2 cDNA, or for Dox-inducible 3F-CD151 (± Dox for 24 hours) were plated on laminin-coated Transwell membranes, and transmembranous migration was evaluated 8 hours later by counting DAPI-stained cells. Representative microscopic fields of GBM1B neurosphere cells transduced with control or CD151 shRNA lentivirus are shown (A; bar = 50 μm). Cells per field were counted (B and C). CD151 silencing inhibited migration and forced CD151 expression promoted migration. (D–J) GBM neurospheres (GBM1A, GBM1B, M1123, 612) infected with lentivirus coding for control shRNA, CD151 shRNA 1, or CD151 shRNA 2 cDNA. 612cells were plated on laminin-coated multiwell nanopatterned devices, and individual cells were tracked using a custom MATLAB program. Average cell speeds at each indicated time point (D) and the overall average speed over a 10-hour time-lapse period (E) are shown. A histogram of average speed for individual cells is shown (F). Average distances migrated over 10 hours were calculated (G). Representative trajectories of cells transduced with control shRNA and CD151 shRNA are shown (H; bar = 100 μm). The start location (red dots) and final locations at 10 hours (blue dots) of individual cells are shown. The green line indicates the path traveled by individual cells. Control cells migrated faster and farther than CD151 shRNA transduced cells. (I and J) Cells were plated on a laminin-coated tissue culture substrata for 2 and 6 hours. Cell adhesion and morphology were evaluated by phase-contrast microscopy (I; bar = 100 μm) and quantified by spectrophotometric analysis of crystal violet–stained cells (J). CD151 silencing inhibited cell spreading and delayed cell adhesion. (K) GBM1A 3F-CD151, GBM1B 3F-CD151, and 612 3F-CD151 neurospheres were treated ± Dox for 24 hours. Cells were dissociated, and adhesion was evaluated by spectrophotometric analysis of crystal violet–stained cells 2 and 6 hours after cells were plated on a laminin-coated surface. CD151 expression promoted adhesion 6 hours after seeding. * $P < .05$ compared with controls.

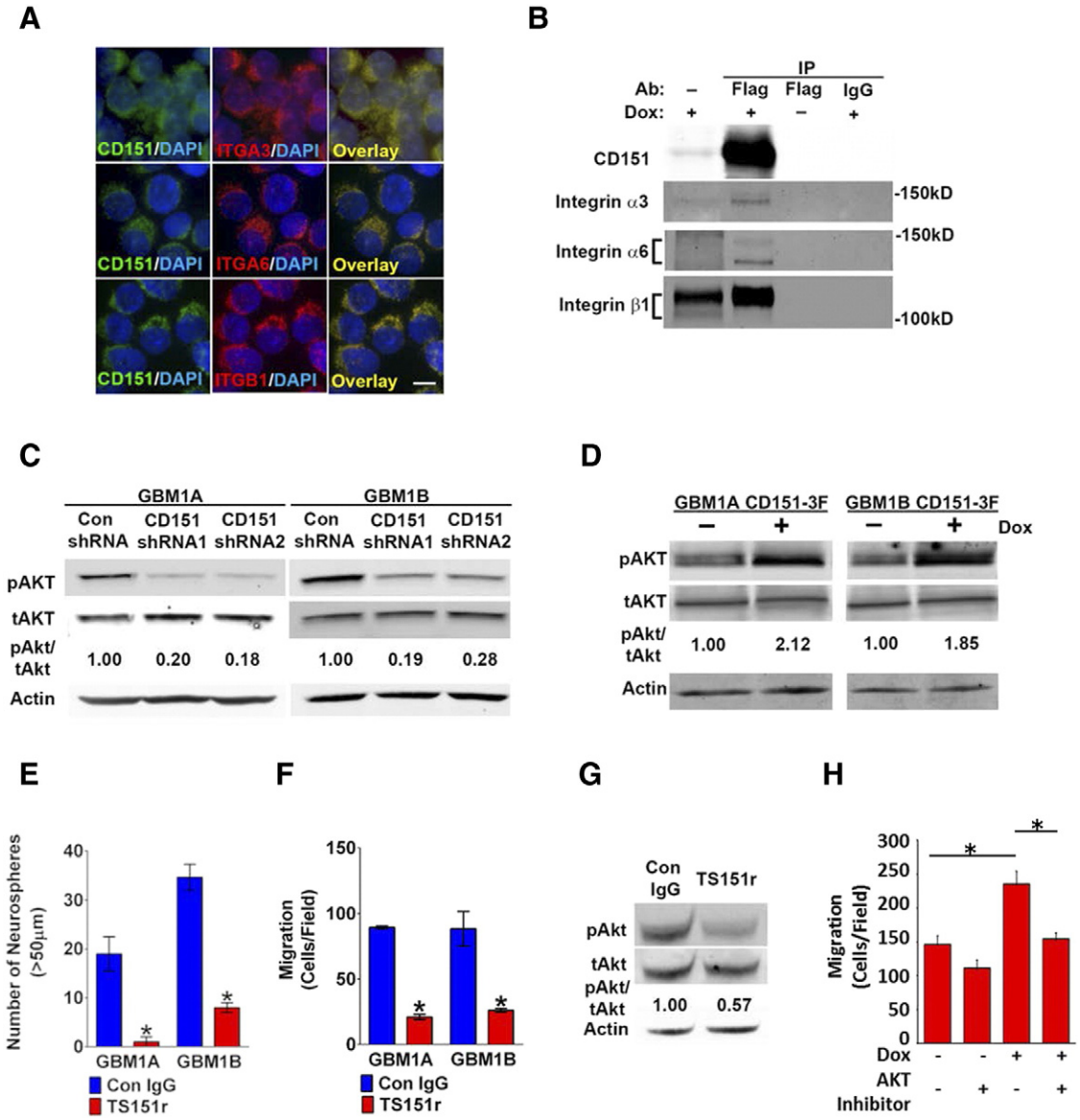

Figure 6. CD151:integrin complexes regulate neurosphere cell self-renewal, migration, and Akt activation.(A) GBM1A neurosphere cells collected by cytospin were co-immunostained with antibodies against CD151 and either integrin α3, integrin α6, or integrin β1 (bar = 10μm). CD151 distribution overlaps with the integrins. (B) GBM1A 3F-CD151 cells were treated ± Dox for 48 hours. Brij-O1 collected protein lysates subjected to immunoprecipitation with anti-FLAG specifically precipitated 3F-CD151, integrin α3, integrin α6, and integrin β1 proteins. (C) GBM neurosphere lines GBM1A and GBM1B were infected with lentivirus coding for control shRNA, CD151 shRNA 1, or CD151 shRNA 2. Total cell lysates were extracted and analyzed by immunoblot using antibodies against S^{473} phosphorylated Akt (pAkt) and total Akt (tAKT). CD151 inhibition decreased Akt phosphorylation. (D) GBM1A 3F-CD151 and GBM1B 3F-CD151 neurospheres were treated ± Dox. Whole cell extracts were analyzed by immunoblot for pAkt and tAkt. Forced CD151 expression promoted Akt phosphorylation. (E–G) GBM1A and GBM1B cells were treated with anti-CD151 antibody TS151r, which blocks integrin α3 and α6 binding. Isotype IgG was used as control. (E) Equal numbers of viable cells were cultured in 48-well plates with TS151r antibody (or IgG control) for 14 days to form neurospheres. Neurospheres (>50 μm diameter) were counted. Neurosphere formation was inhibited by TS151r. (F) Neurosphere cells were plated on laminin-coated Transwell membranes. Migration was evaluated 8 hours later by counting DAPI-stained cells. Cells per field were counted. TS151r inhibited migration on laminin. (G) Whole cell lysates were collected and subjected to immunoblot analysis for pAkt and tAkt. CD151 knockdown inhibits Akt phosphorylation. (H) GBM1A 3F-CD151 cells were treated ± Akt inhibitor MK-2206 (5 μM, Selleckhem, Houston TX) for 1 hour followed by ± Dox for 24 hours to induce 3F-CD151. Neurosphere cells were plated on laminin-coated Transwell membranes. Migration was evaluated 8 hours later by counting DAPI-stained cells. Cells per field were counted. Akt inhibition abrogated CD151-induced cell migration. *P < .01.

Inhibition of GSC-Derived GBM Xenografts by CD151 Silencing

We examined the effects of CD151 silencing on the growth of s.c. and i.c. xenografts established from GBM-derived neurospheres. Subcutaneous xenografts were established in mice with M1123 neurosphere cells engineered to express a Dox-inducible CD151 shRNA (M1123 CD151 shRNA). Beginning on postimplantation day (PID) 8, mice were randomly assigned to control or Dox-treated groups. Tumors were then measured through PID 15 to monitor the effects of CD151 silencing. Average tumor size increased from 74 to

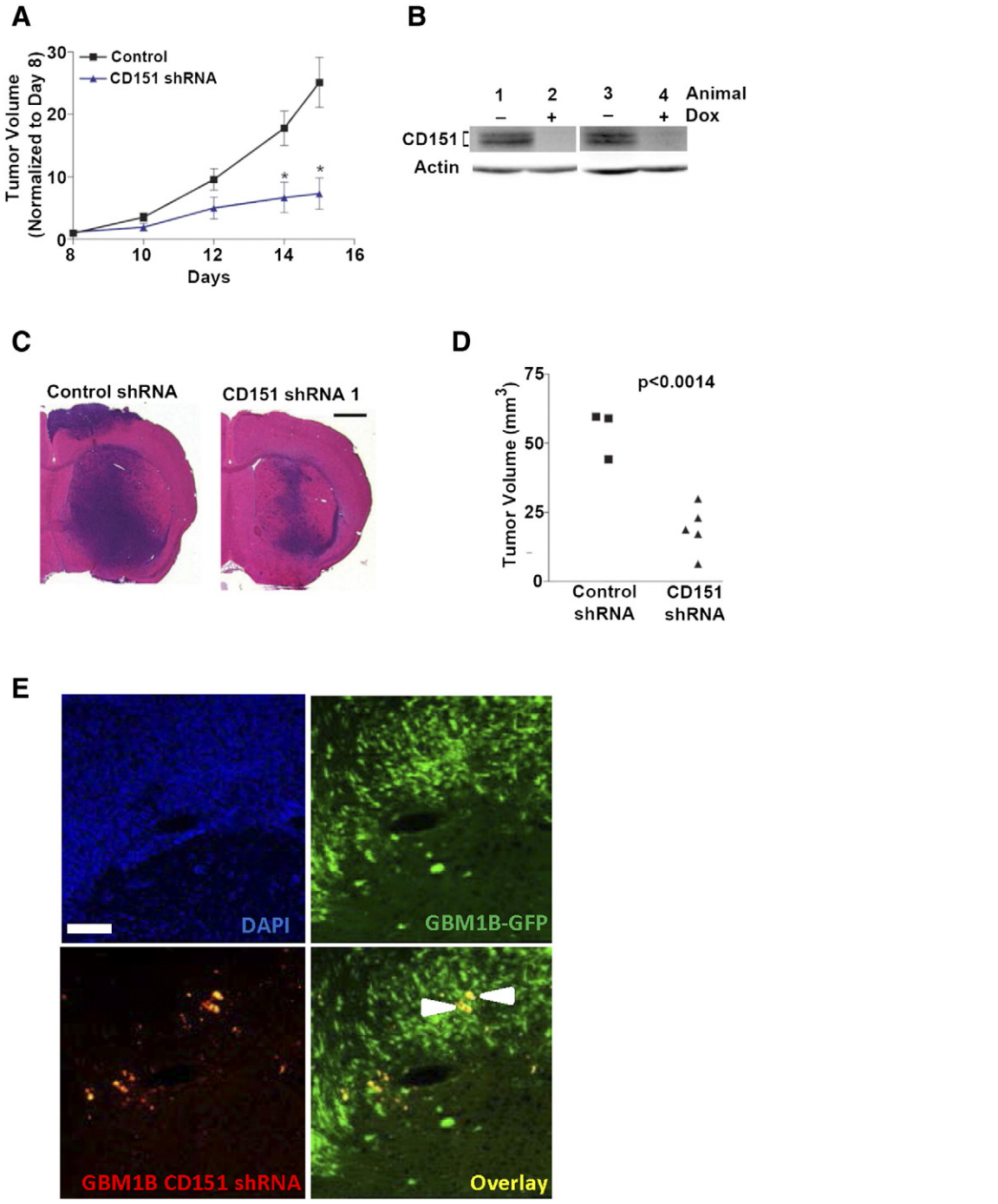

Figure 7. CD151 knockdown inhibits the growth of neurosphere-derived GBM xenografts.(A and B) Mice were implanted subcutaneously with Dox-inducible M1123 CD151 shRNA cells. Mice were started on a Dox-containing diet on PID 8, and tumors were measured daily as described in "Materials and Methods" (A). CD151 knockdown inhibited xenograft growth. Immunoblot analysis of total protein extracts from subcutaneous xenografts obtained on PID 15 confirm *in vivo* Dox-induced CD151 knockdown (B). (C and D) GBM1A cells were transduced with lentivirus coding for control shRNA or CD151 shRNA cDNA. After 24 hours, 5000 viable cells were implanted by stereotactic injection to caudate/putamen of SCID mice. Hematoxylin and eosin–stained coronal brain sections (20 μm) obtained from animals on PID 52 are shown (C; bar = 1 mm). Quantification of xenograft tumor volume shows that silencing CD151 repressed xenograft growth (D; $P < .001$). (E) 10,000 viable GBM1B-GFP control cells and 10,000 viable GBM1B RFP-tagged Dox-inducible CD151 shRNA cells were co-implanted to caudate/putamen of SCID mice. Animals were started on a Dox-containing diet on PID 8 and sacrificed on PID45. Immunofluorescent images of brain sections are shown. The white arrows indicate GBM1B CD151 shRNA cells.

1853 mm^3 in control mice and from 85 to 540 mm^3 in Dox-treated mice. By PID 15, CD151 shRNA had inhibited tumor growth by 71% (Figure 7*A*). CD151 knockdown *in vivo* was confirmed by immunoblot of whole tumor protein extracts using CD151 antibody (Figure 7*B*).

To examine the effect of CD151 silencing on i.c. tumor formation, GBM1A cells were transfected with control lentivirus or with lentivirus expressing CD151 shRNA. Viable cells were implanted 24 hours later into the brains of SCID mice. Mice were

sacrificed 52 days later, and coronal brain sections were examined for tumor size. Tumor formation was significantly reduced in mice implanted with CD151 shRNA-treated cells (19.1 ± 3.9 mm^3 max tumor volume) compared with control shRNA tumors (54.3 ± 5.0 mm^3 max tumor volume) (Figure 7, *C* and *D*).

To further determine the effect of CD151 silencing on tumor formation, GFP-tagged GBM1B control cells and RFP-tagged GBM1B Dox-CD151 shRNA cells were co-implanted to mouse brains. The mice were then treated with Dox for 45 days post–cell implantation. Immunoflourescent imaging of brain sections revealed a marked inhibition of the RFP-tagged CD151 knockdown cells compared with the GFP-tagged controls (Figure 7*E*).

Discussion

Despite recent substantive advances in our understanding of basic cancer mechanisms and their clinical translation, there have been only marginal improvements in the survival of patients with glioblastoma multiforme. This is due at least in part to the specialized biology of glioma-propagating cancer stem cells (GSCs), their resilience in the face of cancer therapies, and their contributions to tumor recurrence. This paper identifies CD151 and its direct interactions with integrins as regulators of GSC stemness and tumorigenicity.

Using multiple approaches, we show that CD151 associates with and actively regulates GSCs and the growth of GBM xenografts derived from GSCs. Glioma neurosphere cells expressing the stemness marker CD133 were found to express high levels of CD151 compared with CD133-negative cells, and silencing CD151 blocked glioma cell capacity to self-renew as spheres, impaired proliferation, and inhibited expression of markers and drivers of cell stemness including CD133, Sox2, and Olig2. Alternatively, CD151 expression was increased in CD133-positive cells following forced expression of the Oct4 and Sox2 transcription factors under conditions that induce glioma-propagating cells [34]. Conversely, forcing the expression of CD151 enhanced glioma cell self-renewal and increased expression of stemness-associated factors. These findings demonstrate a strong mechanistic link between CD151 expression and GSC stemness and provide a novel functional context to our recent report showing that *CD151* resides within a transcriptional network that is repressed by KLF9, a transcription factor that induces GSC differentiation and inhibits GSC tumor-propagating potential. Our data extend and provide a functional context to previous studies from other investigators in different organ systems showing an association of CD151 expression with the capacity of prostate cancer cells to self-renew as spheres [39] and the CD151-dependent regulation of progenitor cell pools during mammary development [58].

Our results point to a cooperative role for the integrin family of cell adhesion receptors that mediate cell-cell and cell–extracellular matrix adhesion interactions and intracellular signaling responses in the mechanism by which CD151 regulates GSCs. Integrins interact with ligands in the extracellular matrix to bidirectionally transduce signals that modulate biological processes, including adhesion and migration [3]. Integrins are also highly expressed in nonneoplastic and neoplastic stem cells and appear to support the stem cell phenotype via interactions with stemness-promoting stromal niches [6,27]. The laminin-binding integrin receptor subunits α3, α6, β1, and β4 in particular have been shown to support GSC stemness. Integrin α3 is upregulated in GSCs and contributes to GSC migration and invasion [36]. Integrin α6 has been found to mark GSCs and regulate GSC self-renewal and tumor-propagating capacity [27].We now show that CD151 directly complexes with integrin receptor subunits α3, α6, and β1 in GBM neurosphere cells and that cell responses activated by forced CD151 expression (i.e., self-renewal as spheres and Akt activation) are inhibited by blocking the CD151-integrin interaction. These findings complement previous studies in other cell models showing that CD151 forms tight complexes with laminin-binding integrins and influences activation of downstream integrin signaling [19,21,43,47,57]. For example, CD151's interaction with integrins α3 and α6 are maintained under stringent lysis conditions (Triton X-100 or NP-40) in melanoma, hepatocellular carcinoma, and endothelial cells [12,19,32]. Liu et al. [32] also showed that overexpression of CD151 activates several downstream proteins in the integrin signaling pathway including FAK, PI3K, Akt, ERK1/2, cdc42, and Rac1 in endothelial cells. Interestingly, we previously found that the transcription factor KLF9, which inhibits GSC stemness and GBM xenograft propagation, represses the expression of both *ita6* (integrin α6) and *CD151*[59]. Thus, CD151 and integrin α6 are co-regulated within a transcriptional network that regulates GSC stemness and glioma propagation.

A prominent feature of clinical gliomas and GSCs is their capacity to invade surrounding brain [42], and CD151 has been shown to promote the adhesion and migratory capacity of several cancer cell types [10,12,24,53,55]. We now show that CD151 stimulates GBM neurosphere cell migration and the rate of neurosphere cell adhesion to integrin-binding substrata. Our data showing that blocking CD151 binding to integrins α3 and α6 inhibits neurosphere cell migration on laminin complement the findings of Fei et al. [12] who found that transfecting hepatocellular carcinoma cells with pAAV-C-D151-AAA, which codes for a mutant CD151 deficient in integrin-binding capacity, inhibits invasion. Similarly, pAAV-C-D151-AAA has been shown to inhibit CD151-promoted cell migration in prostate cancer cells [54].

In conclusion, we show that CD151 supports GBM cell stemness and self-renewal and that inhibiting CD151 expression *in vivo* impedes experimental GBM growth. Our findings directly implicate CD151 binding to integrins α3 and α6 and Akt activation induced by CD151-integrin complex formation in CD151's oncogenic activities. These previously unrecognized CD151 functions suggest alternative approaches to integrin-targeting glioma therapeutics that may be limited by integrin expression on normal neural cells. Our findings support efforts to develop clinically translatable inhibitors of CD151 and CD151-integrin interactions as a potential strategy for targeting GBM tumor-propagating cells and their derivative malignancies.

Supplementary data to this article can be found online at http://dx.doi.org/10.1016/j.neo.2016.02.003.

Acknowledgement

We thank Dr. Ichiro Nakano (Ohio State University) for his kind gift of M1123 and P146 GBM neurosphere lines. This work was partially funded by National Institutes of HealthRO1NS076759 (J. L.) and RO1NS070024 (A. Q. H.), the National Science Foundation Graduate Research Fellowship Program (J. T.), and the Ford Foundation Predoctoral Fellowship Program (J. T.).

References

[1] Abbadi S, Rodarte JJ, Abutaleb A, Lavell E, Smith CL, Ruff W, Schiller J, Olivi A, Levchenko A, and Guerrero-Cazares H, et al (2014). Glucose-6-phosphatase is a key metabolic regulator of glioblastoma invasion. *Mol Cancer Res* **12**, 1547–1559.

[2] Bao S, Wu Q, McLendon RE, Hao Y, Shi Q, Hjelmeland AB, Dewhirst MW, Bigner DD, and Rich JN (2006). Glioma stem cells promote radioresistance by preferential activation of the DNA damage response. *Nature* **444**, 756–760.

[3] Barczyk M, Carracedo S, and Gullberg D (2010). Integrins. *Cell Tissue Res* **339**, 269–280.

[4] Bellail AC, Hunter SB, Brat DJ, Tan C, and Van Meir EG (2004). Microregional extracellular matrix heterogeneity in brain modulates glioma cell invasion. *Int J Biochem Cell Biol* **36**, 1046–1069.

[5] Bredel M, Bredel C, Juric D, Harsh GR, Vogel H, Recht LD, and Sikic BI (2005). Functional network analysis reveals extended gliomagenesis pathway maps and three novel MYC-interacting genes in human gliomas. *Cancer Res* **65**, 8679–8689.

[6] Chen S, Lewallen M, and Xie T (2013). Adhesion in the stem cell niche: biological roles and regulation. *Development* **140**, 255–265.

[7] Cox BD, Natarajan M, Stettner MR, and Gladson CL (2006). New concepts regarding focal adhesion kinase promotion of cell migration and proliferation. *J Cell Biochem* **99**, 35–52.

[8] Deng X, Li Q, Hoff J, Novak M, Yang H, Jin H, Erfani SF, Sharma C, Zhou P, and Rabinovitz I, et al (2012). Integrin-associated CD151 drives ErbB2-evoked mammary tumor onset and metastasis. *Neoplasia* **14**, 678–689.

[9] Detchokul S, Newell B, Williams ED, and Frauman AG (2014). CD151 is associated with prostate cancer cell invasion and lymphangiogenesis *in vivo*. *Oncol Rep* **31**, 241–247.

[10] Devbhandari RP, Shi GM, Ke AW, Wu FZ, Huang XY, Wang XY, Shi YH, Ding ZB, Xu Y, and Dai Z, et al (2011). Profiling of the tetraspanin CD151 web and conspiracy of CD151/integrin beta1 complex in the progression of hepatocellular carcinoma. *PLoS One* **6**e24901.

[11] Dolecek TA, Propp JM, Stroup NE, and Kruchko C (2012). CBTRUS statistical report: primary brain and central nervous system tumors diagnosed in the United States in 2005-2009. *Neuro-Oncology* **14**(Suppl. 5), v1–v49.

[12] Fei Y, Wang J, Liu W, Zuo H, Qin J, Wang D, Zeng H, and Liu Z (2012). CD151 promotes cancer cell metastasis via integrins alpha3beta1 and alpha6beta1 in vitro. *Mol Med Rep* **6**, 1226–1230.

[13] Feng Y, Zhu M, Dangelmajer S, Lee YM, Wijesekera O, Castellanos CX, Denduluri A, Chaichana KL, Li Q, and Zhang H, et al (2014). Hypoxia-cultured human adipose-derived mesenchymal stem cells are non-oncogenic and have enhanced viability, motility, and tropism to brain cancer. *Cell Death Dis* **5**e1567.

[14] Feng Y, Zhu M, Dangelmajer S, Lee YM, Wijesekera O, Castellanos CX, Denduluri A, Chaichana KL, Li Q, and Zhang H, et al (2015). Hypoxia-cultured human adipose-derived mesenchymal stem cells are non-oncogenic and have enhanced viability, motility, and tropism to brain cancer. *Cell Death Dis* **6**e1797.

[15] Galli R, Binda E, Orfanelli U, Cipelletti B, Gritti A, De Vitis S, Fiocco R, Foroni C, Dimeco F, and Vescovi A (2004). Isolation and characterization of tumorigenic, stem-like neural precursors from human glioblastoma. *Cancer Res* **64**, 7011–7021.

[16] Gangemi RM, Griffero F, Marubbi D, Perera M, Capra MC, Malatesta P, Ravetti GL, Zona GL, Daga A, and Corte G (2009). SOX2 silencing in glioblastoma tumor-initiating cells causes stop of proliferation and loss of tumorigenicity. *Stem Cells* **27**, 40–48.

[17] Garzon-Muvdi T, Schiapparelli P, ap Rhys C, Guerrero-Cazares H, Smith C, Kim DH, Kone L, Farber H, Lee DY, and An SS, et al (2012). Regulation of brain tumor dispersal by NKCC1 through a novel role in focal adhesion regulation. *PLoS Biol* **10**e1001320.

[18] Gemei M, Di Noto R, Mirabelli P, and Del Vecchio L (2013). Cytometric profiling of CD133+ cells in human colon carcinoma cell lines identifies a common core phenotype and cell type-specific mosaics. *Int J Biol Markers* **28**, 267–273.

[19] Hong IK, Jeoung DI, Ha KS, Kim YM, and Lee H (2012). Tetraspanin CD151 stimulates adhesion-dependent activation of Ras, Rac, and Cdc42 by facilitating molecular association between beta1 integrins and small GTPases. *J Biol Chem* **287**, 32027–32039.

[20] Ignatova TN, Kukekov VG, Laywell ED, Suslov ON, Vrionis FD, and Steindler DA (2002). Human cortical glial tumors contain neural stem-like cells expressing astroglial and neuronal markers in vitro. *Glia* **39**, 193–206.

[21] Kazarov AR, Yang X, Stipp CS, Sehgal B, and Hemler ME (2002). An extracellular site on tetraspanin CD151 determines alpha 3 and alpha 6 integrin-dependent cellular morphology. *J Cell Biol* **158**, 1299–1309.

[22] Kim DH, Han K, Gupta K, Kwon KW, Suh KY, and Levchenko A (2009). Mechanosensitivity of fibroblast cell shape and movement to anisotropic substratum topography gradients. *Biomaterials* **30**, 5433–5444.

[23] Kim DH, Seo CH, Han K, Kwon KW, Levchenko A, and Suh KY (2009). Guided cell migration on microtextured substrates with variable local density and anisotropy. *Adv Funct Mater* **19**, 1579–1586.

[24] Klosek SK, Nakashiro K, Hara S, Shintani S, Hasegawa H, and Hamakawa H (2005). CD151 forms a functional complex with c-Met in human salivary gland cancer cells. *Biochem Biophys Res Commun* **336**, 408–416.

[25] Kondapalli KC, Llongueras JP, Capilla-Gonzalez V, Prasad H, Hack A, Smith C, Guerrero-Cazares H, Quinones-Hinojosa A, and Rao R (2015). A leak pathway for luminal protons in endosomes drives oncogenic signalling in glioblastoma. *Nat Commun* **6**, 6289.

[26] Lal B, Xia S, Abounader R, and Laterra J (2005). Targeting the c-Met pathway potentiates glioblastoma responses to gamma-radiation. *Clin Cancer Res* **11**, 4479–4486.

[27] Lathia JD, Gallagher J, Heddleston JM, Wang J, Eyler CE, Macswords J, Wu Q, Vasanji A, McLendon RE, and Hjelmeland AB, et al (2010). Integrin alpha 6 regulates glioblastoma stem cells. *Cell Stem Cell* **6**, 421–432.

[28] Lee D, Suh YL, Park TI, Do IG, Seol HJ, Nam DH, and Kim ST (2013). Prognostic significance of tetraspanin CD151 in newly diagnosed glioblastomas. *J Surg Oncol* **107**, 646–652.

[29] Lee J, Kotliarova S, Kotliarov Y, Li A, Su Q, Donin NM, Pastorino S, Purow BW, Christopher N, and Zhang W, et al (2006). Tumor stem cells derived from glioblastomas cultured in bFGF and EGF more closely mirror the phenotype and genotype of primary tumors than do serum-cultured cell lines. *Cancer Cell* **9**, 391–403.

[30] Li Q, Wijesekera O, Salas SJ, Wang JY, Zhu M, Aprhys C, Chaichana KL, Chesler DA, Zhang H, and Smith CL, et al (2014). Mesenchymal stem cells from human fat engineered to secrete BMP4 are nononcogenic, suppress brain cancer, and prolong survival. *Clin Cancer Res* **20**, 2375–2387.

[31] Li Y, Li A, Glas M, Lal B, Ying M, Sang Y, Xia S, Trageser D, Guerrero-Cazares H, and Eberhart CG, et al (2011). c-Met signaling induces a reprogramming network and supports the glioblastoma stem-like phenotype. *Proc Natl Acad Sci U S A* **108**, 9951–9956.

[32] Liu WF, Zuo HJ, Chai BL, Peng D, Fei YJ, Lin JY, Yu XH, Wang DW, and Liu ZX (2011). Role of tetraspanin CD151-alpha3/alpha6 integrin complex: implication in angiogenesis CD151-integrin complex in angiogenesis. *Int J Biochem Cell Biol* **43**, 642–650.

[33] Lobo NA, Shimono Y, Qian D, and Clarke MF (2007). The biology of cancer stem cells. *Annu Rev Cell Dev Biol* **23**, 675–699.

[34] Lopez-Bertoni H, Lal B, Li A, Caplan M, Guerrero-Cazares H, Eberhart CG, Quinones-Hinojosa A, Glas M, Scheffler B, and Laterra J, et al (2015). DNMT-dependent suppression of microRNA regulates the induction of GBM tumor-propagating phenotype by Oct4 and Sox2. *Oncogene* **34**(30), 3994–4004.

[35] McGirt MJ, Than KD, Weingart JD, Chaichana KL, Attenello FJ, Olivi A, Laterra J, Kleinberg LR, Grossman SA, and Brem H, et al (2009). Gliadel (BCNU) wafer plus concomitant temozolomide therapy after primary resection of glioblastoma multiforme. *J Neurosurg* **110**, 583–588.

[36] Nakada M, Nambu E, Furuyama N, Yoshida Y, Takino T, Hayashi Y, Sato H, Sai Y, Tsuji T, and Miyamoto KI, et al (2013). Integrin alpha3 is overexpressed in glioma stem-like cells and promotes invasion. *Br J Cancer* **108**, 2516–2524.

[37] Novitskaya V, Romanska H, Dawoud M, Jones JL, and Berditchevski F (2010). Tetraspanin CD151 regulates growth of mammary epithelial cells in three-dimensional extracellular matrix: implication for mammary ductal carcinoma in situ. *Cancer Res* **70**, 4698–4708.

[38] Peng D, Zuo H, Liu Z, Qin J, Zhou Y, Li P, Wang D, Zeng H, and Zhang XA (2013). The tetraspanin CD151-ARSA mutant inhibits angiogenesis via the YRSL sequence. *Mol Med Rep* **7**, 836–842.

[39] Rajasekhar VK, Studer L, Gerald W, Socci ND, and Scher HI (2011). Tumour-initiating stem-like cells in human prostate cancer exhibit increased NF-kappaB signalling. *Nat Commun* **2**, 162.

[40] Rao Malla R, Gopinath S, Alapati K, Gorantla B, Gondi CS, and Rao JS (2013). Knockdown of cathepsin B and uPAR inhibits CD151 and alpha3beta1 integrin-mediated cell adhesion and invasion in glioma. *Mol Carcinog* **52**, 777–790.

[41] Serru V, Le Naour F, Billard M, Azorsa DO, Lanza F, Boucheix C, and Rubinstein E (1999). Selective tetraspan-integrin complexes (CD81/alpha4beta1, CD151/alpha3beta1, CD151/alpha6beta1) under conditions disrupting tetraspan interactions. *Biochem J* **340**(Pt 1), 103–111.

[42] Sever R and Brugge JS (2015). Signal transduction in cancer. *Cold Spring Harb Perspect Med* **5**(4).

[43] Sincock PM, Fitter S, Parton RG, Berndt MC, Gamble JR, and Ashman LK (1999). PETA-3/CD151, a member of the transmembrane 4 superfamily, is localised to the plasma membrane and endocytic system of endothelial cells, associates with multiple integrins and modulates cell function. *J Cell Sci* **112**, 833–844.

[44] Singh SK, Clarke ID, Terasaki M, Bonn VE, Hawkins C, Squire J, and Dirks PB (2003). Identification of a cancer stem cell in human brain tumors. *Cancer Res* **63**, 5821–5828.

[45] Singh SK, Hawkins C, Clarke ID, Squire JA, Bayani J, Hide T, Henkelman RM, Cusimano MD, and Dirks PB (2004). Identification of human brain tumour initiating cells. *Nature* **432**, 396–401.

[46] Smith CL, Chaichana KL, Lee YM, Lin B, Stanko KM, O'Donnell T, Gupta S, Shah SR, Wang J, and Wijesekera O, et al (2015). Pre-exposure of human adipose mesenchymal stem cells to soluble factors enhances their homing to brain cancer. *Stem Cells Transl Med* **4**, 239–251.

[47] Sterk LM, Geuijen CA, van den Berg JG, Claessen N, Weening JJ, and Sonnenberg A (2002). Association of the tetraspanin CD151 with the laminin-binding integrins alpha3beta1, alpha6beta1, alpha6beta4 and alpha7-beta1 in cells in culture and *in vivo*. *J Cell Sci* **115**, 1161–1173.

[48] Stiles CD and Rowitch DH (2008). Glioma stem cells: a midterm exam. *Neuron* **58**, 832–846.

[49] Tilghman J, Wu H, Sang Y, Shi X, Guerrero-Cazares H, Quinones-Hinojosa A, Eberhart CG, Laterra J, and Ying M (2014). HMMR maintains the stemness and tumorigenicity of glioblastoma stem-like cells. *Cancer Res* **74**, 3168–3179.

[50] Vescovi AL, Galli R, and Reynolds BA (2006). Brain tumour stem cells. *Nat Rev Cancer* **6**, 425–436.

[51] Visvader JE and Lindeman GJ (2008). Cancer stem cells in solid tumours: accumulating evidence and unresolved questions. *Nat Rev Cancer* **8**, 755–768.

[52] Voss MA, Gordon N, Maloney S, Ganesan R, Ludeman L, McCarthy K, Gornall R, Schaller G, Wei W, and Berditchevski F, et al (2011). Tetraspanin CD151 is a novel prognostic marker in poor outcome endometrial cancer. *Br J Cancer* **104**, 1611–1618.

[53] Winterwood NE, Varzavand A, Meland MN, Ashman LK, and Stipp CS (2006). A critical role for tetraspanin CD151 in alpha3beta1 and alpha6beta4 integrin-dependent tumor cell functions on laminin-5. *Mol Biol Cell* **17**, 2707–2721.

[54] Yang W, Li P, Lin J, Zuo H, Zuo P, Zou Y, and Liu Z (2012). CD151 promotes proliferation and migration of PC3 cells via the formation of CD151-integrin alpha3/alpha6 complex. *J Huazhong Univ Sci Technolog Med Sci* **32**(3), 383–388.

[55] Yang XH, Richardson AL, Torres-Arzayus MI, Zhou P, Sharma C, Kazarov AR, Andzelm MM, Strominger JL, Brown M, and Hemler ME (2008). CD151 accelerates breast cancer by regulating alpha 6 integrin function, signaling, and molecular organization. *Cancer Res* **68**, 3204–3213.

[56] Yang YM, Zhang ZW, Liu QM, Sun YF, Yu JR, and Xu WX (2013). Overexpression of CD151 predicts prognosis in patients with resected gastric cancer. *PLoS One* **8**e58990.

[57] Yauch RL, Kazarov AR, Desai B, Lee RT, and Hemler ME (2000). Direct extracellular contact between integrin alpha(3)beta(1) and TM4SF protein CD151. *J Biol Chem* **275**, 9230–9238.

[58] Yin Y, Deng X, Liu Z, Baldwin LA, Lefringhouse J, Zhang J, Hoff JT, Erfani SF, Rucker III EB, and O'Connor K, et al (2014). CD151 represses mammary gland development by maintaining the niches of progenitor cells. *Cell Cycle* **13**, 2707–2722.

[59] Ying M, Tilghman J, Wei Y, Guerrero-Cazares H, Quinones-Hinojosa A, Ji H, and Laterra J (2014). Kruppel-like factor-9 (KLF9) inhibits glioblastoma stemness through global transcription repression and integrin alpha6 inhibition. *J Biol Chem* **289**, 32742–32756.

[60] Zheng ZZ and Liu ZX (2007). Activation of the phosphatidylinositol 3-kinase/protein kinase Akt pathway mediates CD151-induced endothelial cell proliferation and cell migration. *Int J Biochem Cell Biol* **39**, 340–348.

[61] Zheng ZZ and Liu ZX (2007). CD151 gene delivery increases eNOS activity and induces ECV304 migration, proliferation and tube formation. *Acta Pharmacol Sin* **28**, 66–72.

[62] Zhu M, Feng Y, Dangelmajer S, Guerrero-Cazares H, Chaichana KL, Smith CL, Levchenko A, Lei T, and Quinones-Hinojosa A (2015). Human cerebrospinal fluid regulates proliferation and migration of stem cells through insulin-like growth factor-1. *Stem Cells Dev* **24**, 160–171.

[63] Zoller M (2009). Tetraspanins: push and pull in suppressing and promoting metastasis. *Nat Rev Cancer* **9**, 40–55.